Morphology Selection of Nanoparticle Dispersions by Polymer Media

Jaeup U. Kim[1] and Ben O'Shaughnessy[2]

[1]*Department of Physics, Columbia University, New York, New York 10027*
[2]*Department of Chemical Engineering, Columbia University, New York, New York 10027*

Designable media can control properties of nanocomposite materials by spatially organizing nanoparticles. Here we theoretically study particle organization by ultrathin polymer films of grafted chains ("brushes"). Polymer-soluble nanoparticles smaller than a brush-determined threshold disperse in the film to a depth scaling inversely with particle volume. In the polymer-insoluble case, aggregation is directed: provided particles are nonwetting at the film surface, the brush stabilizes the dispersion and selects its final morphology of giant elongated aggregates with a brush-selected width.

The prospect of a new generation of materials and devices based on the assembly of nanoparticles into spatially extended 2D and 3D arrangements is a major driving force in the rapidly emerging field of nanoscale research [1,2]. Nanoparticles, the "designer molecules" governing the macroscopic behavior of these novel materials, can be constructed according to a vast range of design principles, promising unprecedented tuning of material properties. Both for technology and for fundamental research in condensation matter physics, the implications are far reaching.

This Letter addresses a major challenge in the field: how to spatially organize the nanoparticles. The interparticles *medium* plays a crucial role in this regard, and one would like to "design" media to achieve different spatial arrangements leading to different interparticle couplings and entirely different macroscopic properties. Much recent research has examined polymeric media spontaneously forming nanostructured phases as templates for particle organization [1–4]. Moreover, polymer-particle composites are often conveniently processable with important implication for thin film and other technologies [2,5,6].

In this Letter, we develop a systematic theory of ultrathin polymer films as organizing media to achieve 2D nanoparticle arrangements. The latter are central to information storage media applications and of fundamental importance to 2D electronic phenomena. We are directly motivated by recent studies of metallic and semiconducting nanoparticles in films of end-tethered polymer chains [5] forming "polymer brushes," and in diblock copolymer materials whose lamellae offer a similarly 2D brushlike environment [3,6]. A major objective is that this work offer guidance to such experiments by identifying the key physical variables to achieve nanoparticle dispersions and control morphology.

Given a nanoparticle-containing film of substrate-grafted polymer chains of N units at grafting density σ [Fig. 1(a)] in contact with air, we will see there are two distinct classes of behavior depending on whether the particles are (A) soluble or (B) insoluble in the free polymer medium (ungrafted chains). Our principle conclusions are as follows:

(A) For *polymer-soluble* particles (well compatibilized) their size b is crucial: (i) Sufficiently small particles disperse freely within the polymer brush film. (ii) Above a threshold size b^*, equilibrium particle penetration is limited to a depth δ and the film has a loading capacity $\phi_{\max}$. Both δ and the maximum particle density $\phi_{\max}$ scale inversely with particle volume b^3. (iii) Particles larger than a second threshold $b_{\max} \approx (N/\sigma)^{1/4}$ cannot penetrate the film.

(B) *Polymer-insoluble* particles tend to aggregate in the polymer film, of course. This aggregation is *directed* by the polymer brush: (i) The brush imposes a severe free energy penalty for aggregate growth in two lateral directions simultaneously (parallel to substrate) and aggregates tend to be anisotropic. (ii) As growth continues, aggregates are expelled towards the brush-air interface and the final state depends on the polymer-nanoparticle-air interfacial tensions. If the nanoparticles tend to wet the polymer film surface, they will spread to form a near
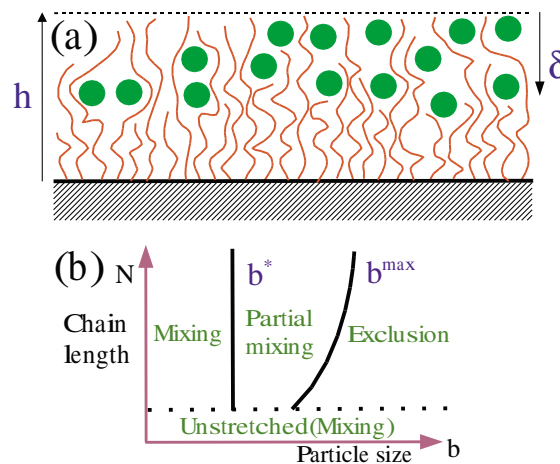

FIG. 1 (color online). (a) Schematic of polymer film containing nanoparticles in contact with air. (b) Phase diagram for polymer-soluble nanoparticles [case (A)].

monolayer. In the nonwetting case, growth is ultimately arrested and the final morphology consists in large elongated aggregates, embedded in the film, whose width is selected by the brush.

Note that for case (B) the experimental procedure must forcibly introduce the nanoparticles into the polymer film. Once inside, we find that extremely large barriers effectively stabilize their presence in the film and prevent phase separation. For nonwetting particles, the brush *selects the morphology* of giant anisotropic nanoparticle aggregates with a selected lateral dimension. The physical origin of these effects is that aggregates extended in two lateral directions impose radical distortions on brush chain configurations (see Figs. 2 and 3), whereas chains are relatively undistorted by an aggregate elongated in only one direction, around which they can "flow" by taking the shortest route. This costs much less free energy.

For the remainder of this Letter, we briefly outline our calculations leading to these conclusions. In typical grafted polymer films, chain end anchoring is achieved by attaching an end block chemically similar to the substrate [5]. It is well known that as grafting density increases, brush height h increases [see Fig. 1(a)] due to incompressibility, $h = \sigma N$, and chains are forced to stretch. A Gaussian chain has stretching energy $h^2/2N$
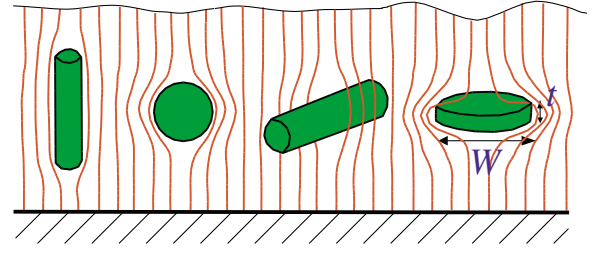
$$F = \int d\boldsymbol{\rho} g(\boldsymbol{\rho}) \frac{3}{2} \int_0^N dn \left(\frac{\partial \mathbf{R}}{\partial n}\right)^2 + \int d\mathbf{r} P(\mathbf{r})[\phi_{\text{pol}}(\mathbf{r}) + \phi_{\text{nano}}(\mathbf{r}) - 1] + F_{\text{nano}}[\phi_{\text{nano}}], \tag{1}$$

where $\phi_{\text{pol}}(\mathbf{r}) \equiv \int d\boldsymbol{\rho} g(\boldsymbol{\rho}) \int_0^N dn \delta[\mathbf{r} - \mathbf{R}(n, \boldsymbol{\rho})]$ is the polymer density and $g(\boldsymbol{\rho})$ is the distribution of chain end locations $\boldsymbol{\rho}$, $\mathbf{R}(0, \boldsymbol{\rho}) \equiv \boldsymbol{\rho}$. The first term represents chain stretching free energy [8], the pressurelike field $P(\mathbf{r})$ enforces incompressibility, and F_{nano} describes interactions involving nanoparticles.

Now, if one deletes the nanoparticle terms, this gives the free energy considered by Semenov for the pure non-solvated brush [8]. Semenov found that in the free-energetically favored brush configuration chain ends are distributed throughout the brush, i.e., the "Alexander–de Gennes" picture in which all ends lie at height h is wrong. Correspondingly, the pressure field is quadratic, $P(z) = (3\pi^2/4)[P_0(1 - z^2/h^2)]$.

Extending Semenov's analysis, we minimize F with respect to both polymer plus nanoparticle fields. At moderate volume fractions $F_{\text{nano}} \simeq \int d\mathbf{r} (\phi_{\text{nano}}/b^3) \ln(\phi_{\text{nano}}/e)$ is dominated by translational entropy and we find

$$\phi_{\text{nano}}(z) = \phi_{\text{nano}}(h) e^{-P(z)b^3}, \tag{2}$$

where the pressure field remains quadratic but the substrate pressure and brush height are increased. Noting that the pressure vanishes at the brush surface $z = h$, and is approximately linear for small depths, we write $\phi_{\text{nano}}(z) \sim e^{-(h-z)/\delta}$ where $\delta \equiv h(b^*/b)^3$ and $b^* \approx (N/h)^{2/3} = 1/\sigma^{2/3}$. Thus for $b \gg b^*$ the penetration depth $\delta \sim 1/b^3$ is much less than the full height. It de-

FIG. 2 (color online). The degree an inclusion disrupts a polymer brush depends strongly on shape and orientation. The free energy cost ΔF is least for vertically oriented cylinders. A disk is much more disruptive and ΔF is amplified by the disk aspect ratio W/t.

[7], leading to a brush stretching energy density or "pressure" $P_0 = (1/2)(h/N)^2 = \sigma^2/2$. (Units are chosen so kT and monomer size are unity.)

Now suppose nanoparticles are forced into such a brush; typically these are surface-stabilized metallic, metal oxide, or semiconductor nanocrystals [2,3,6]. We first consider polymer-soluble particles, case (A). To determine nanoparticle distributions $\phi_{\text{nano}}(\mathbf{r})$ within the brush, our starting point is the following brush free energy as a function of chain configurations $\mathbf{R}(n, \boldsymbol{\rho})$ [n is the monomer label, $0 \leq n \leq N$, $\mathbf{r} \equiv (x, y, z)$ with z orthogonal to the substrate]:

creases with increasing particle size until $\delta = b$ defines the maximum sized particle $b = b_{\text{max}} \approx (N/\sigma)^{1/4}$ which can enter the brush. In the partial penetration regime, $b^* < b < b_{\text{max}}$, the maximum particle volume fraction is $\phi_{\text{max}} = \delta/h \sim 1/b^3$. Above this level, excess nanoparticles are expelled outside [9].

These results are represented in Fig. 1(b). Their physical origin is clear. Because of Semenov's chain end relaxation effect, the brush edge is much softer than
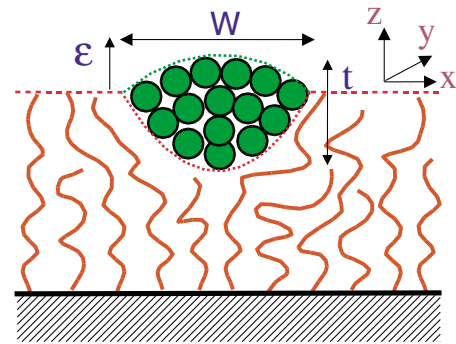

FIG. 3 (color online). To minimize its free energy a nanoparticle aggregate at the polymer film-air interface chooses a baguette shape of length L in the y direction (perpendicular to the plane of the paper). Its cross section comprises two half lenses above and below the film surface.

elsewhere and pressure increases monotonically from the free brush surface: the brush tends to push particles towards its surface. Mixing entropy opposes this, and the penetration depth δ is obtained by balancing the entropy, of order kT, with $P(\delta)b^3$, the particle's chain stretching energy penalty at depth δ.

Let us now turn to case (B), nanoparticles insoluble in the polymer, i.e., the nanoparticle-polymer interfacial tension γ_{np} (see below) exceeds a critical (positive) value. After being forced into the brush, van der Waals attractions coalesce them into increasingly large aggregates [5]. Our previous analysis, which treated nanoinclusions as fluidlike perturbations, is not adequate for large inclusions. Among previous works addressing this intrinsically nonperturbative problem [10,11], in an important contribution Williams and Pincus [12] proved an object in a strongly stretched brush is analogous to irrotational steady state inviscid flow past the same object. Polymer configurations map to flow streamlines, and brush energy equals fluid kinetic energy [12].

Exploiting this analogy, by using flow solutions past various objects [13] we calculated the brush energy cost ΔF for nanoparticles to form aggregates of different sizes and shapes (see Fig. 2) for aggregate size much less than h. We find that momentum conservation in the hydrodynamic analogy translates to the statement that for a given aggregate volume Ω there is a baseline free energy cost of exactly $2P_0\Omega$. Additional cost depends on shape: $\Delta F = 2P_0\Omega$ and $3P_0\Omega$ for cylinders perpendicular and parallel to the substate, respectively; $\Delta F = (5/2)P_0\Omega$ for spheres; and $\Delta F = (4/3\pi)P_0\Omega(W/t)$ for disks of diameter W and thickness t. Note the much greater cost for disks due to the aspect ratio factor $W/t \gg 1$.

While suggestive, these results are not quite conclusive since the hydrodynamic analogy applies only to the simplified Alexander–de Gennes brush [12]. Thus we attempted to extend our results to an aggregate at height z in the true end-annealed brush. We find

$$\Delta F = P(z)\Omega \quad \text{(vert. cylinder)},$$
$$\Delta F = \alpha P(z)\Omega \quad \text{(sphere)}, \qquad (3)$$
$$\Delta F = \beta P(z)\Omega \quad \text{(horiz. cylinder)},$$

where $1 < \alpha < 5/4$ and $1 < \beta < 3/2$ are constants. Regardless of shape, we find that "fluidizing" the aggregate in the x, y directions to infinity always lowers ΔF. This leads to a rigorous lower bound, $\Delta F \geq P(z)\Omega$. The upper bounds were obtained by constructing a brush configuration from a superposition of hydrodynamiclike solutions, each corresponding to a different value of chain end location ρ [cf. Eq. (1)]. This configuration satisfies incompressibility exactly. We calculated its (shape-dependent) free energy. However, this is not the true global energy minimum. It thus provides a rigorous upper bound to ΔF, as shown in Eq. (3). We conclude that the effect of end annealing is to replace $2P_0$ with the pressure $P(z)$ at the aggregate location and, for spheres and cylin-

ders, to modify prefactors. We cannot rigorously conclude the same for disks for which we find an upper bound $\Delta F < (2/3\pi)P(z)\Omega(W/t)$. However, given our result for the Alexander–de Gennes brush, we conjecture that the same is true for disks: $\Delta F = \gamma P(z)\Omega (W/t)$ where $\gamma < (2/3\pi)$. Note that vertically elongated aggregates are favored, due to brush-induced effective interactions between nanoparticles which are dipolelike, entirely analogous to the doublets of hydrodynamics [13].

These results also tell us elongation in one lateral direction (horizontal cylinder shape) invokes little penalty, whereas the brush strongly opposes simultaneous growth in two lateral directions (disklike, Fig. 2). Thus, as aggregation proceeds and sizes reach order h, further growth can continue in one horizontal direction only. However, aggregates larger than h can always reduce their free energy by accessing the polymer-air interface. The final state thus hinges on the three relevant surface tensions: γ_{np} (nanoaggregate-polymer), γ_{na} (nanoaggregate-air), and γ_{pa} (polymer-air). These determine the familiar [14] *spreading coefficient* $S \equiv \gamma_{pa} - \gamma_{np} - \gamma_{na}$ and *entry coefficient* $E \equiv \gamma_{pa} + \gamma_{np} - \gamma_{na}$. Now it is well known [14] that a droplet on a simple liquid surface assumes a lens shape to minimize its free energy. In the present case, where the liquid is a viscoelastic brush, we find the generalization of this result is that the nanoparticle aggregate forms a baguette shape at the polymer-air interface of length L (y direction) with lens-shaped cross section of width W (x direction) bulging a depth $t - \epsilon$ into the brush and ϵ into the air. This is illustrated in Fig. 3. The baguette free energy reads

$$\Delta F = \frac{P_0 L W^3 (t - \epsilon)^2}{h^3} f_1(L/W) - SLW f_2(L/W)$$
$$+ \left[\gamma_{na} \frac{L\epsilon^2}{W} + \gamma_{np} \frac{L(t - \epsilon)^2}{W} \right] f_3(L/W). \qquad (4)$$

The first term is the brush stretching energy penalty for a surface depression of depth $t - \epsilon$, width W, and length L [11]; the second results from the baguette displacing an area LW of air-polymer interface; and the last two from extra surface area created by each half lens. The factors $f_i \equiv \alpha_i + \beta_i W/L$ add extra areas due to the baguette's end caps (located at $y = 0, L$) where α_i, β_i are constant geometric factors of order unity.

Next we minimize the free energy per unit volume for an ensemble of aggregates, $\Delta F/\Omega$ [where $\Omega = LWt(A + BW/l)$ with A, B constants]. We find (i) if $S > 0$ (i.e., nanoparticles *wet* the polymer material) an infinite nanoparticle monolayer spreads onto the polymer film surface, $L, W \to \infty$, $\epsilon = t \to 0$. Physically, there is no advantage in penetrating the brush because droplet entry into the polymer-air interface is favored since $E > 0$ (since $E > S$ when $\gamma_{np} > 0$). (ii) If $S < 0$ and $E > 0$, then $W = W^* \approx \delta^{1/4} h \approx h$ since $\delta^{1/4}$ is typically close to unity, t is also of order h, $L \to \infty$, and $\epsilon \to 0$. That is, nanoaggregates grow freely in one lateral direction but

the brush stabilizes growth in the other, selecting a characteristic width W^*. (We find a similar stabilization in the slightly more complex case of $E < 0$.) This is actually a metastable state; however, we find that provided the air surface tensions (γ_{na}, γ_{pa}) are much larger than γ_{np} the barrier separating this state from true phase separation is of height $|S|\delta_{na}^{1/2}h^2$ where $\delta_{na} \equiv \gamma_{na}/P_0 h$. This is usually extremely high, since typically $\delta_{na}^{1/2}$ and $|S|$ are of order unity or greater and $h^2 \gg 1$. Even without this barrier, the air medium is likely to strongly inhibit particle fluidization and prevent phase separation.

We also performed a more complete analysis accounting for fluctuations. We find width fluctuations $\delta w \approx |S|^{-1/2}$, baguette persistence length $l_p \approx |S|W^{*3}$, and mean baguette length $\overline{L} \sim \phi^{1/2}e^{F_{cap}}$, where ϕ is interface nanoparticle areal fraction and $F_{cap} \approx |S|W^{*2}$ the baguette end-cap free energy.

A number of experiments and numerical works have addressed nanoparticle organization by polymeric media. The workers of Ref. [3] studied PS(polystyrene)-coated Fe_2O_3 nanoparticles in lamellar PS-PBMA diblock materials. Neutron specular reflection data suggested 6 nm nanoparticles remain near the PS center plane while 4 nm particles penetrate into the PS layer, possibly accessing the PS-PBMA interface. In numerical work by Balazs and co-workers [4] equations were solved describing lamellar diblocks with nanoparticles soluble in one polymer species [case (A)]. We estimate (b/b^*) values of 2 and 1.3, suggesting the partial mixing regime (see Fig. 1). Consistent with this, nanoparticle density profiles peaked at and decayed away from the lamellar center plane. We stress, however, that the above experimental and numerical systems involve diblock lamellar structures. Though the chain stretching physics is expected to be similar, these are more complex than the brush case studied here since new features associated with partitioning between the diblock species are involved. A few thin film systems have been studied [2,5]. In Ref. [5], TEM images of PEP(polyethylenepropylene)-insoluble [case (B)] dodecanethiol-stabilized gold nanoparticles of size 2.5 nm in PEP thin film brushes ($h = 13$ nm) show nanoparticles apparently macroscopically phase separated into film surface monolayers, suggesting $S > 0$. Our theory then predicts no shape and size selection. For $h = 5$ nm elongated aggregates with a characteristic width were observed. In this situation, not dealt with by our theory, grafting density is so low that the film is thinner than the coil radius R_g so chains are not stretched but instead collapsed.

In summary, ultrathin films of end-tethered polymers can actively organize nanoparticles to produce novel composite materials. The polymer medium generates effective anisotropic interactions between nanoparticles, directing aggregate growth and determining the morphology of the nanoparticle dispersion. The origin of these effects is that the stretching energy cost for polymer brush chains depends strongly on aggregate shape. Our theory suggests two alternative strategies for mixing nanoparticles into polymer brushes or lamellar phases. (i) Compatibilize particles to be soluble in the polymer medium and synthesize them as small as possible; particles above a certain size ($b > b_{max}$) will simply not remain within the film. For example, with $h/R_g = 2$ where $R_g = N^{1/2}$ is the unperturbed polymer coil size [5] one has $b_{max} \approx R_g/3 \approx 3$ nm for monomer size 0.3 nm and $N = 1000$. (ii) To stabilize giant elongated aggregates embedded in the film but near its surface, nanoparticles should be insoluble in the polymer and nonwetting on the polymer surface ($S < 0$). Thus, as important as the nanoparticle design is the design of the polymer medium whose incompatibility with air (or whichever is the third medium) should be minimized. To guarantee a stable morphology the polymer should be less incompatible with air than the nanoparticles are ($\gamma_{pa} < \gamma_{na}$).

[1] V. Z. -H. Chan et al., Science **286**, 1716 (1999); T. Thurn-Albrecht et al., Science **290**, 2126 (2000).

[2] D. E. Fogg et al., Macromolecules **30**, 8433 (1997).

[3] B. Hamdoun, D. Auserre, V. Cabuil, and S. Joly, J. Phys. II (France) **6**, 503 (1996); V. Lauter-Pasyuk et al., Physica (Amsterdam) **241B–243B**, 1092 (1998).

[4] R. B. Thompson, V. V. Ginzburg, M. W. Matsen, and A. C. Balazs, Science **292**, 2469 (2001); J. Huh, V. V. Ginzburg, and A. C. Balazs, Macromolecules **33**, 8085 (2000).

[5] Z. Liu et al., Nanoletters **2**, 219 (2002).

[6] R. W. Zehner et al., Langmuir **14**, 241 (1998); J. F. Ciebien, R. T. Clay, B. H. Sohn, and R. E. Cohen, New J. Chem. **22**, 685 (1998); B. Lin et al., J. Appl. Phys. **85**, 3180 (1999).

[7] P.-G. de Gennes, *Scaling Concepts in Polymer Physics* (Cornell University Press, Ithaca, New York, 1979).

[8] A. N. Semenov, Sov. Phys. JETP **61**, 733 (1985).

[9] In the soluble case, for simplicity we assumed particles are nonwetting on the brush surface ($S < 0$).

[10] F. J. Solis, Macromolecules **29**, 4060 (1996); F. J. Solis and H. Tang, *ibid.* **29**, 7953 (1996).

[11] G. H. Fredrickson, A. Ajdari, L. Leibler, and J. Carton, Macromolecules **25**, 2882 (1992).

[12] D. R. M. Williams and P. A. Pincus, Europhys. Lett. **24**, 29 (1993).

[13] H. Lamb, *Hydrodynamics* (Dover Publications, New York, 1945).

[14] I. Langmuir, J. Chem. Phys. **1**, 756 (1933); P. R. Pujado and L. E. Scriven, J. Colloid Interface Sci. **40**, 82 (1972).